

Prestenotic Bronchial Radioaerosol Deposition: A New Ventilation Scan Sign of Bronchial Obstruction

Soo-Kyo Chung, Hak-Hee Kim and Yong-Whee Bahk

Departments of Radiology and Nuclear Medicine, Kangnam St. Mary's Hospital, Catholic University Medical College, Seoul, Korea; and Department of Radiology, Samsung Cheil General Hospital, Seoul, Korea

This study was performed to assess the diagnostic usefulness of aerosol ventilation scanning in bronchial obstruction and bronchial stenosis. **Methods:** Seven patients of bronchial obstruction and one patient with stenosis were studied. In each patient, obstruction was confirmed by bronchography, bronchoscopy and/or CT scan. Ventilation scanning was performed using the ^{99m}Tc -phytate aerosol generated by a BARC jet nebulizer. Scan manifestations were assessed in correlation with those of plain chest radiography, bronchography, CT scan and/or bronchoscopy. **Results:** In every patient, the ventilation scan showed characteristic intense aerosol deposition in a short, slightly dilated, clubbed, bronchial segment immediately proximal to obstruction or stenosis. Typically, it was accompanied by a distal airspace deposition defect. **Conclusion:** Intense, segmental, bronchial aerosol deposition with distal lung defect was a specific finding of bronchial obstruction and stenosis. The sign was especially useful when obstruction was obscured by the associated, bizarre lung disease and in a small bronchus.

Key Words: bronchial obstruction; radioaerosol deposition; ventilation scan; technetium-99m-phytate

J Nucl Med 1997; 38:71-74

Bronchial obstruction, an important airway pathology, frequently imposes a diagnostic problem not only clinically but also plain radiographically. The specific, radiographic sign of bronchial obstruction is the direct demonstration of "occluded bronchial lumen," which is not readily achievable on plain radiograph. Thus, it is customary to diagnose a bronchial obstruction by noting indirect signs such as vascular crowding, consolidation and shift of anatomical landmarks. Clearly, these signs do not indicate an obstruction, but a lung collapse that may result from many nonobstructive causes such as compression, fibrosis and surfactant deficiency (1). Plain radiographic detection of an obstruction is difficult when it is incomplete with confusing air trapping in the distal airspace (1,2). The diagnosis becomes harder still when obstruction is associated with and obscured by bizarre lung disease, which is a common occurrence as shown in the present series. In such a situation, even a CT scan may not be of value unless slices accurately include the small, short obstruction site and separate it from the associated lung disease. Bronchography and bronchoscopy are accurate but obviously invasive. The diagnostic usefulness of ventilation scan using ^{133}Xe gas or ^{81m}Kr gas in obstructive pulmonary disease has been well-documented (2,3), and the test was found to be superior to plain chest radiography in detecting small bronchus obstruction because it would produce scan defects that were easy to observe (2). Obviously, however, such a scan defect is not specific since it can also be produced by several nonobstructive lung diseases such as pneumonia, edema

and tumor. Nor does it directly indicate obstruction as a ^{99m}Tc -phytate aerosol scan does.

In the course of the recent ventilation scan studies on bronchial obstruction using ^{99m}Tc -phytate aerosol, we observed a previously unrecognized interesting phenomenon. It was characterized by an intense, short, segmental aerosol deposition in the immediate prestenotic bronchus, accurately pointing to obstruction and stenosis. The aerosol-deposited bronchus appeared to be slightly dilated and clubbed and was accompanied by a scan defect in the distal lung.

METHODS

We studied five men (age 31–69 yr) and two women (age 61 and 69 yr) with eight lesions. One male patient with pulmonary tuberculosis had obstructions in both upper lobe bronchi. The obstruction was complete in seven patients and incomplete with stenosis in one. The obstruction site was sublobar in three patients, lobar in four and in the main-stem bronchus in one. The causes were chronic nonspecific inflammation ($n = 3$), tuberculosis ($n = 4$) and small-cell carcinoma with tuberculosis ($n = 1$). The gold standard for diagnosis was confirmatory evidences of bronchial obstruction on conventional x-ray tomography, CT scan, bronchography and/or bronchoscopy and histology where necessary. Ventilation scan alterations were correlated to those results in addition to plain chest radiographic alterations such as vascular crowding and increased density of collapsed lung.

Aerosol scanning was performed after inhalation, in a resting tidal breathing state, of submicronic aerosol of ^{99m}Tc -phytate through a mask for 5 min in a sitting position (4,5). The inhaled radioactivity was approximately 3 mCi (111 MBq). The aerosol was generated afresh each time by using a BARC nebulizer (Bhabha Atomic Research Center, Bombay, India) after instillation of 15 mCi (555 MBq) ^{99m}Tc -phytate. The activity median aerodynamic diameter (AMAD) of aerosols was estimated to be $0.84\ \mu\text{m}$, with σ (GSD) being 1.71 (6). After rinsing the esophagus, scanning was performed with the subject lying on a scan couch, and images were acquired in the anterior, posterior and both lateral positions. A total of 500K counts was accumulated over a period of 8 min per view, which was nearly twice the recommended count of 300K. This was to improve image quality by setting the filter at the near baseline level to suppress the sensitivity of the detector.

RESULTS

In the seven patients with bronchial obstruction and the one patient with stenosis, bronchial obstruction was clearly indicated by an intense, segmental, aerosol deposition in the immediate, prestenotic bronchus (Figs. 1, 2). Characteristically, it was short, minimally dilated, clubbed in appearance and accompanied by a deposition defect in the distal airspace that was reduced in volume in obstruction and overinflated in stenosis. On the other hand, the plain chest radiograph showed the obstruction site in only one patient in whom the main-stem bronchus was involved (Fig. 3A). In all other patients, the site of obstruction could not be delineated, although there were

Received Dec. 29, 1995; revision accepted May 29, 1996.

For correspondence or reprints contact: Yong-Whee Bahk, MD, PhD, FFAST, Senior Consultant, Department of Radiology, Samsung Cheil General Hospital, Seoul 100-380, Korea.

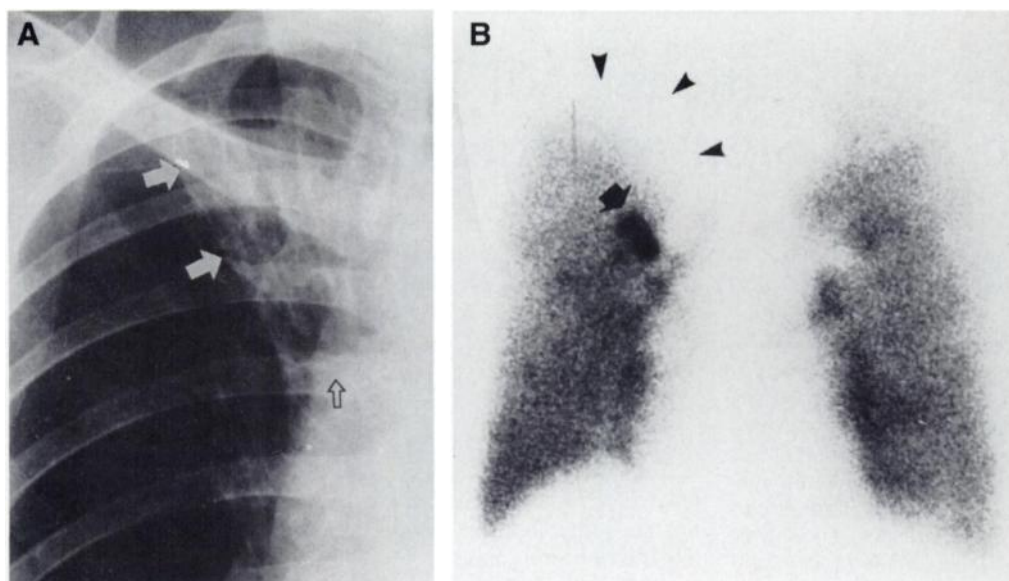


FIGURE 1. Typical, prestenotic aerosol deposition in a 57-yr-old man with a right upper lobe bronchus obstruction due to tuberculosis. (A) Posteroanterior right upper chest radiograph shows increased density with crowded vascular markings of collapsed lung (arrows) and cranially shifted hilum (open arrow). Obstruction is not depicted. (B) Anterior aerosol scan reveals intense tracer deposition in the clubbed, dilated, prestenotic, right upper lobe bronchus (arrow). Also, note a large deposition defect in the collapsed, right upper lobe (arrowheads).

indirect suggestions of obstruction such as increased lung density, crowded vascular markings and shifting of the hilar and mediastinal structures. The increased density of collapsed lung was either obvious (Figs. 1A, 3A) or unimpressive (Figs. 4A, 5A). It was either partially or totally obscured by the associated lung disease, overlying heart and/or mediastinal structures, thereby preventing its accurate delineation. For example, the chest radiograph of one patient with chronic inflammatory obstruction of the medial segment of the middle lobe showed inconclusive evidence of pathology, but the aerosol scan showed the characteristic, intense, prestenotic aerosol deposition, which clearly indicated bronchial obstruction (Fig. 5).

DISCUSSION

Bronchial obstruction is one of the most common airway disorders created by several causes, including inflammation, tuberculosis, mucus plug, foreign body, trauma and tumors. Bronchial obstruction may be either complete or incomplete. Its accurate diagnosis is imperative, but it is often not easily achievable without resorting to invasive procedures such as bronchography and bronchoscopy or costly CT scan, which is not always confirmatory when the involved bronchus is not large enough or is obscured by the associated lung lesions. The standard diagnostic approach is plain chest radiography followed by conventional x-ray tomography, bronchography, CT scan or bronchoscopy. Generally, the plain chest radiography is useful, but it cannot specifically delineate the obstruction site except when a heavy-penetration technique is used in occasional cases of obstruction in a larger bronchus (Fig. 3A).

Regardless of the size of the bronchus involved, the specific diagnosis is even more difficult when obstruction is obscured by a bizarre, associated lung lesion such as tuberculosis, chronic inflammation and fibrosis. As shown in the present series, it is a rather common clinical occurrence. When an obstruction involves a smaller bronchus, the diagnostic accuracy and success rate will become further reduced.

In the vast majority of bronchial obstructions, plain radiographic diagnosis relies on the demonstration of indirect signs such as increased density, crowding of vascular markings and shifting of anatomical landmarks (Figs. 1A–5A). Evidently, when a small bronchus is involved, these signs become unreliable, and when obstruction is incomplete the lung may look normal (3). As previously mentioned, these signs may become readily obscured by the associated and superimposed lung disease. All these facts distract the value of plain radiography. Also of note is that the lung consolidation resulted from bronchial obstruction, which often disguises pneumonia (Fig. 6), and when such a consolidation hides in the cardiac or mediastinal shadow, the diagnosis becomes confusing. It is in these situations that aerosol scanning can play a decisive role.

The usefulness of ^{133}Xe gas or $^{81\text{m}}\text{Kr}$ gas ventilation scan in obstructive pulmonary disease has been described (2,3), and the test was found to be superior to plain chest radiography in detecting small bronchus obstruction because the scan would produce a readily recognizable defect while the radiograph looked normal (2). It is obvious, however, that such a scan defect is not specific and can also be produced by airspace

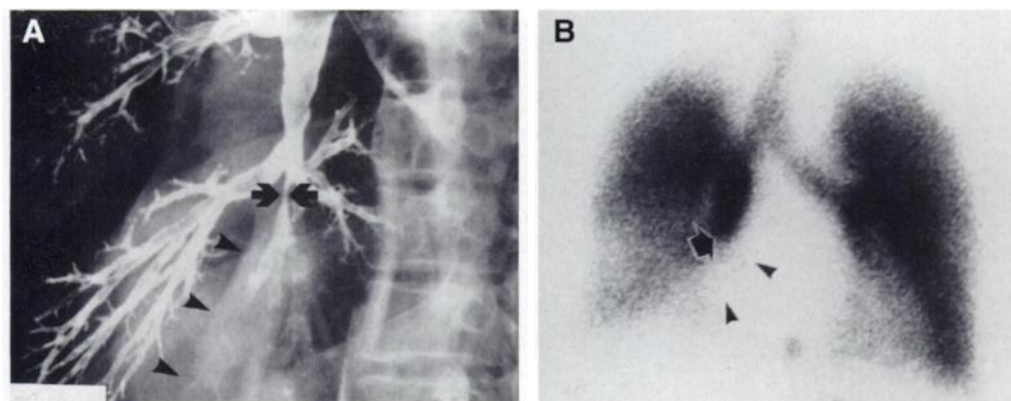


FIGURE 2. Intense, prestenotic aerosol deposition in bronchial stenosis due to chronic inflammation. (A) Left anterior oblique view of the right bronchography shows narrowing of the proximal, right lower lobe bronchus (arrows) with lung collapse (arrowheads). (B) Anterior aerosol scan reveals intense tracer deposition in the clubbed, dilated, prestenotic, intermediate bronchus (arrow) with accompanying deposition defect (arrowheads).

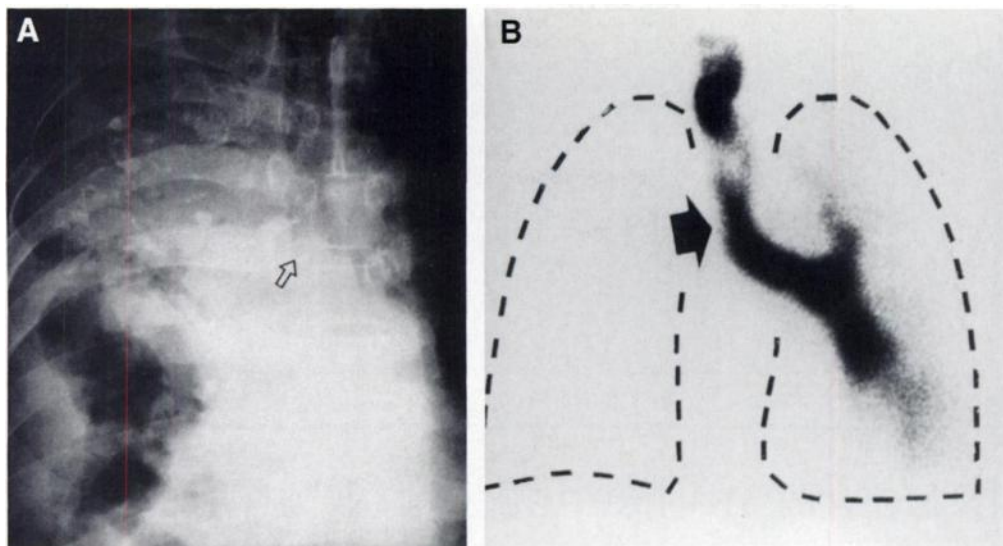


FIGURE 3. Modified, prestenotic aerosol deposition in the trachea in a 69-yr-old man with advanced tuberculosis and right main-stem bronchus carcinoma. (A) High-penetration, posteroanterior chest radiograph shows obstruction (open arrow). (B) Anterior aerosol scan reveals complete obstruction of the right main-stem bronchus with an intense tracer deposition in the trachea and left main-stem bronchus due to tracheal damage, disturbed transport and excess of aerosols, respectively (arrow). This is considered to be a case of modified, prestenotic aerosol deposition.

diseases such as pneumonia, edema and tumor without a bronchial obstruction. Neither do ^{133}Xe and $^{81\text{m}}\text{Kr}$ scans directly indicate an obstruction site as does a $^{99\text{m}}\text{Tc}$ -phytate aerosol scan. Our series demonstrates that the aerosol scan has a definite place in detecting bronchial obstruction and stenosis, especially when it is in a sublobar bronchus (Fig. 2) or obscured by bizarre, associated lung disease (Fig. 3). Thus, regardless of bronchial size and the presence of obscuring lung disease, the site was clearly indicated by an intense, short, segmental aerosol deposition in the prestenotic bronchus (Figs. 1B–5B). The affected bronchus appeared to be clubbed and slightly dilated and was accompanied by the distal scan defect in the collapsed or emphysematous lung. While the characteristic scan sign was seen in all eight patients studied, plain radiography was either inconclusive or indirect at best in all but one patient with cancer in the right main-stem bronchus (Fig. 3).

The mechanism by which such a peculiar aerosol deposition takes place in the immediate, prestenotic bronchus is speculative. However, it may be due to chronic bronchial wall damage and hindered mucociliary movement with resultant hold-up of aerosol migration (7). Such an aerosol deposition in the ob-

struction site of the lung has been related to turbulent bronchial air flow (8). In this connection, it is interesting that Boxen and Zhang (9) ascribed the diffuse aerosol deposition in the major airways noted in tracheobronchitis to a similar mechanism.

CONCLUSION

Technetium-99m-phytate aerosol scanning of bronchial obstruction and stenosis demonstrated intense tracer deposition in the immediate, prestenotic bronchus which was slightly dilated and clubbed in appearance. Typically, it was accompanied by a distal airspace deposition defect. The sign appears to be specific, and we propose naming it “the prestenotic aerosol deposition sign.”

ACKNOWLEDGMENTS

The BARC nebulizer was generously donated by the International Atomic Energy Agency, Vienna, under the provision of Coordinated Research Program (Contract no. 302-E1-ROK-4819). This study was also supported in part by the Clinical Research

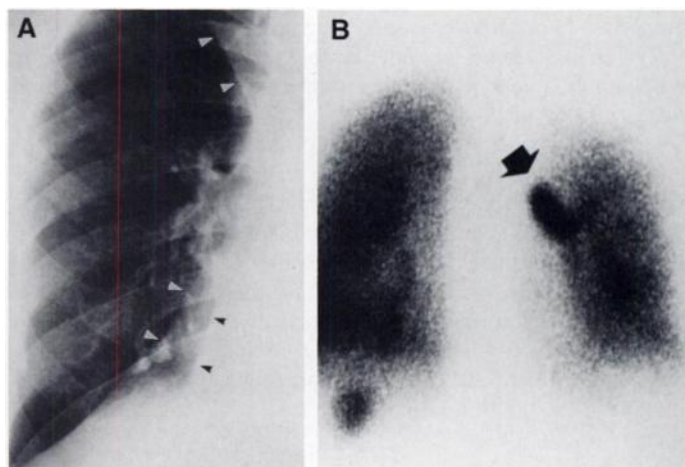


FIGURE 4. Intense, prestenotic aerosol deposition in radiographically obscure bronchial obstruction in a 31-yr-old man with chronic inflammation. (A) Posteroanterior right chest radiograph shows barely discernible, double, triangular opacities of collapsed middle lobe (lower, white arrowheads) and lower lobe (black arrowheads). Both are obscured by the cardiac shadow. Obstruction is not shown. Note the upper triangular sign, an indirect sign of lower lung collapse (upper, white arrowheads). (B) Posterior aerosol scan reveals the classic, prestenotic tracer deposition in the intermediate bronchus that is clubbed and dilated (arrow).

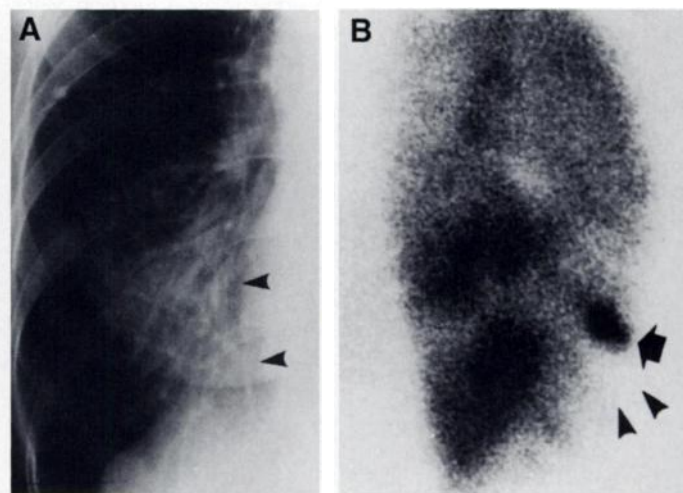


FIGURE 5. Decisive role of aerosol scanning in sublobar, bronchial obstruction in a 61-yr-old woman with chronic pneumonia in the medial segment of the right middle lobe. (A) Posteroanterior right lower chest radiograph shows an inconclusive density in the right paracardiac region (arrowheads). Obstruction is not shown. (B) Right lateral aerosol scan reveals intense tracer deposition in the proximal middle lobe bronchus (arrow) with accompanying deposition defect in the distal lung (arrowheads).

Fund of Catholic University Medical College, Seoul, Korea. We thank Mr. Tae-Sung Choi, NMRT for fine aerosol imaging, Mr. Hee-Duk Roh for photographic work and Miss Nam-Jee Joo for administrative assistance.

REFERENCES

1. Fraser RG, Paré JAP. Parenchymal atelectasis. In: Fraser RG, Paré JAP, eds. *Diagnosis of diseases of the chest*. Philadelphia: W. B. Saunders; 1977:353-377.
2. Lavender JP, Irving H, Armstrong JD II. Krypton-81m ventilation scanning: acute respiratory disease. *Am J Roentgenol* 1981;136:309-316.
3. Alderson PO, Secker-Walker RH, Forrest JV. Detection of obstructive pulmonary disease. *Radiology* 1974;111:643-648.
4. Kotrappa P, Raghunath B, Subramanyam PPS, et al. Scintigraphy of lungs with dry aerosol-generation and delivery system. *J Nucl Med* 1977;18:1082-1085.
5. Soni PS, Raghunath B. Generation of aerosols: BARC nebulizer and others. In: Bahk YW, Isawa T, eds. *Radioaerosol imaging of the lung*. Vienna: International Atomic Energy Agency Publication; 1994:24-42.
6. Bahk YW, Chung SK. Radioaerosol lung scanning in chronic obstructive pulmonary disease (COPD) and related disorders. In: Bahk YW, Isawa T, eds. *Radioaerosol imaging of the lung*. Vienna: International Atomic Energy Agency Publication; 1994:88-135.
7. Isawa T, Teshima T, Hirano T, et al. Mucociliary clearance and transport in bronchiectasis: global and regional assessment. *J Nucl Med* 1990;31:543-548.
8. Hayes M, Taplin GV. Lung imaging with radioaerosols for the assessment of airway disease. *Semin Nucl Med* 1980;10:243-251.
9. Boxen I, Zhang ZM. Deposition of radioaerosol throughout the major airways in tracheobronchitis. *Clin Nucl Med* 1990;15:703-704.

Background Subtraction in Technetium-99m-MAG3 Renography

Andrew Taylor, Jr, Killol Thakore, Russell Folks, Raghuveer Halkar and Amita Manatunga

Division of Nuclear Medicine, Department of Radiology, Emory University School of Medicine, Atlanta, Georgia; and Louisiana State University Medical Center, New Orleans, Louisiana

Correction represents a potential source of error in estimating split renal function and camera-based clearances. The purpose of this study was to determine which of five background options and four time intervals was associated with the least error for ^{99m}Tc -mercaptoacetyltriglycine (MAG3). **Methods:** Fifteen single-kidney patients were imaged supine after 111-370 MBq (3-10 mCi) ^{99m}Tc -MAG3 injection. A phantom kidney was drawn on the 2-3-min images, approximately equal in size to the solitary kidney and used for all time intervals. Counts in the phantom and native kidneys were calculated using manual inferior and lateral regions of interest (ROIs), automated elliptical and perirenal background ROIs and no background correction at various time intervals (1-2, 1-2.5, 1.5-2.5 and 2-3 min) postinjection. With optimal background correction, counts and the relative function in the phantom kidney should be zero. The error was measuring by estimating both the relative function and absolute function expressed as the percent injected dose in the phantom kidney. **Results:** The percent injected dose in the phantom kidney as well as the error in measuring relative function were significantly greater than zero for the inferior background correction and the no background correction options at all time intervals, $p < 0.05$. The percent dose in the kidney and the error associated with the lateral, elliptical and perirenal ROIs were not significantly different from zero. **Conclusion:** Regardless of time interval, the greatest error was associated with no background correction. The inferior ROI consistently underestimated the background correction and probably should not be used for ^{99m}Tc -MAG3. There was no significant difference between errors generated using the lateral and automated ROIs, although automated ROIs are probably more reproducible for sequential studies.

Key Words: background correction; relative renal function; regions of interest

J Nucl Med 1997; 38:74-79

Radionuclide renograms should routinely include a measurement of relative renal function (1-3). Most commercial software programs make this measurement during the 1-2- or 2-3-min interval after radiopharmaceutical injection. Moreover,

camera-based methods are available to calculate the glomerular filtration rate (GFR), effective renal plasma flow (ERPF) and ^{99m}Tc -mercaptoacetyltriglycine (MAG3) clearance based on the percent of the injected dose of ^{99m}Tc -diethylenetriamine-pentaacetic acid (DTPA), [^{131}I]ortho-iodohippurate (OIH) or MAG3 in the kidneys at 1-2, 1-2.5 or 2-3 min postinjection (4-6). Measurements of relative renal function and gamma camera based clearance measurements are usually corrected for background and results may differ depending on the background region selected. Controversy exists not only with the method and region of interest (ROI) used for background correction but also whether or not background subtraction is even needed (2,7-11). Some authors suggest that, at relative good levels of renal function, the use of background subtraction introduces more problems than it solves and that it is virtually impossible, short of removing the kidney, to determine the true background contribution in any given individual at a given time (2,9). Finally, results obtained with ^{99m}Tc -DTPA or OIH may not be applicable to MAG3 due to its higher protein binding and lower volume of distribution.

To better evaluate the most appropriate background ROI for patients undergoing ^{99m}Tc -MAG3 renography, a study was done to estimate relative renal function in a series of 15 patients with unilateral nephrectomies. A phantom kidney was drawn approximately equal in size to the solitary kidney. The goal of the study was to evaluate the effects of various background options (no background, elliptical, perirenal, inferior and lateral backgrounds) on both the relative function and the ^{99m}Tc -MAG3 clearance in the phantom kidney at various time intervals postinjection (1-2, 1-2.5, 1.5-2.5 and 2-3 min, respectively).

MATERIALS AND METHODS

Following intravenous administration of 3-10 mCi (111-370 MBq) ^{99m}Tc -MAG3, images were acquired posteriorly at 2 sec/frame for 24 frames, 15 sec/frame for 16 frames and 30 sec/frame for 40 frames with patients in the supine position. Data were acquired using a gamma camera equipped with 400 mm crystal and a low-energy, all-purpose, parallel-hole (LEAP) collimator and processed using the QuantEMTM software (Emory

Received June 20, 1995; revision accepted June 22, 1996.

For correspondence or reprints contact: Andrew Taylor, Jr, MD, Division of Nuclear Medicine, Department of Radiology, Emory University School of Medicine, 1364 Clifton Rd., NE, Atlanta, GA 30322.